Constraints on the redshift dependence of the dark energy potential

Joan Simon,* Licia Verde,† and Raul Jimenez‡

Dept. of Physics and Astronomy, University of Pennsylvania, 209 South 33rd Street, Philadelphia, Pennsylvania 19104, USA
(Received 10 December 2004; published 16 June 2005)

We develop a formalism to characterize the shape and the redshift evolution of the dark energy potential. Our formalism makes use of quantities similar to the horizon-flow parameters in inflation and is general enough that can deal with multiscalar quintessence scenarios, exotic matter components, and higher-order curvature corrections to General Relativity. We show how the shape of the dark energy potential can be recovered nonparametrically using this formalism and we present approximations analogous to the ones relevant to slow-roll inflation. Since presently available data do not allow a nonparametric and exact reconstruction of the potential, we consider a general parametric description. This reconstruction can also be used in other approaches followed in the literature (e.g., the reconstruction of the redshift evolution of the dark energy equation of state $w(z)$). Using observations of passively evolving galaxies and supernova data we derive constraints on the dark energy potential shape in the redshift range $0.1 < z < 1.8$. Our findings show that at the 1σ level the potential is consistent with being constant, although at the same level of confidence variations cannot be excluded with current data. We forecast constraints achievable with future data from the Atacama Cosmology Telescope.

I. INTRODUCTION

Recent observations [1,2] indicate that $\simeq 70\%$ of the present-day energy density of the Universe may be made of a dark energy component. The two leading explanations of dark energy are a cosmological constant or a slowly rolling scalar field, e.g., [3–7], but an explanation in terms of modifications to the Friedman equations, e.g., [8,9], is also possible. In both cases this component has a negative pressure thus inducing an accelerated expansion of the Universe.

A significant observational effort is directed to unveil the nature of dark energy (e.g. [10–15]).

The strongest constraints to date on the nature of dark energy measure the integrated value over time of its equation of state parameter ($w = \rho/p$) (e.g., [1,2,16–18]). These constraints are very tight (e.g. [2] finds $w = -0.98 \pm 0.12$) and are centered around the expected value for the cosmological constant, but, as pointed out by [19,20], the finding that the time average value of w is consistent with -1 does not exclude the possibility that w varied in time. Therefore, it is an open challenge to determine whether dark energy is a cosmological constant or a rolling of a scalar field. A recent review of the current status of our knowledge of the observational determination of w and possible theoretical models to explain it is given by [3].

Recently, observational data sets, or combinations of different data sets, became powerful enough to attempt to constrain a possible redshift dependence $w(z)$ (e.g., [1,21] or, alternatively, to trace the dark energy density as a function of time (e.g., [22–27]); since the dark energy density depends on an integral over $w(z)$, to obtain the dark energy density as a function of z one effectively needs to take one derivative of e.g., luminosity distance measurements but effectively 2 derivatives to obtain $w(z)$ thus $\rho(z)$ can be constrained more directly from observational data e.g., [28–30].

From a theoretical point of view, it is not only important to clarify whether the energy component is dynamical or constant, but, in case it is not a cosmological constant, it is also of great interest to constrain the shape of the potential of the rolling scalar field. Since different theoretical models are typically characterized by different potentials, a reconstruction of the dark energy potential from observations can yield more direct constraints on physically motivated dark energy models.

In this paper we take a different approach and attempt to reconstruct directly the dark energy potential; since theoretical models directly predicts the shape of the dark energy potential this makes comparison with theory more straightforward. In [31], a different reconstruction for the quintessence potential was suggested in terms of the present fraction in dark energy, the present equation of state, and the amount of early dark energy. In our formalism, we attempt instead to reconstruct such potential directly, in terms of the Hubble parameter and dark matter density, in general cases, but in terms of the Hubble parameter alone in the presence of simple dark matter.

We first present a nonparametric method to reconstruct the redshift evolution of the potential and kinetic energy of the dark energy field. Our formalism introduces quantities similar to the horizon-flow parameters [32,33] in inflation. It has the nice feature that it is easily implemented in the presence of higher-order curvature corrections to General Relativity and different types of energy contributions in

―――――――――
*Electronic address: jsimon@bokchoy.hep.upenn.edu
†Electronic address: lverde@physics.upenn.edu
‡Electronic address: raulj@physics.upenn.edu

Einstein's equations, as we do in Section II A. Our exact reconstruction formulas determine the value of the potential at a given redshift once the matter density, Hubble parameter (H), and its first derivative ($\dot{H}$) are experimentally measured at that redshift value and, in principle, yield exact reconstruction of higher-order derivatives of the potential. We discuss the observational challenges to reconstruct the potential in this fully nonparametric way due to the difficulty of measuring $\dot{H}$. As current data is not good enough to determine $\dot{H}$, we present a general parametrization of the potential, based on an expansion in Chebyshev polynomials. In this approach, the scalar potential as a function of redshift is expanded in Chebyshev polynomials, which constitutes a complete orthonormal basis on a finite interval, and have the nice property to be the *minimax* approximating polynomial. Our reconstruction equation becomes a differential equation for the Hubble parameter, which we solve analytically, and the coefficients in the Chebyshev expansion become the parameters to be constrained from observations of the Hubble parameter. Our general parametrization can apply to other approaches that were already considered in the literature, such as expansions of the equation of state and we show the correspondence to some parametrizations that have been proposed in the literature. Using current data (in particular relative ages of a sample of passively evolving galaxies and recent supernovae data) we reconstruct the potential of dark energy using our parametrization up to $z \sim 1.8$. The reconstructed potentials obtained from galaxy ages and SN are consistent. Since these two data sets rely on independent physics and are affected by completely different systematics, this finding suggests that possible systematics are not a crucial issue.

The reconstructed potential is consistent with being constant up to the maximum redshift of the observations, although current constraints do not exclude a variation as a function of redshift. We show that data obtained with the Atacama Cosmology Telescope will be able to greatly improve current constraints.

II. METHOD

A. Dynamics of the scalar field of dark energy

The classical effective action that we shall use to describe the dynamics of the Universe is

$$S = \int dt\, d^3x \sqrt{-g} \left\{ -\frac{m_p^2}{16\pi}(R + f(R, R^{\mu\nu}R_{\mu\nu}, \ldots) \right.$$
$$\left. + \frac{g^{\mu\nu}}{2} \partial_\mu q \partial_\nu q - V(q) \right\} + S_{\text{sources}}, \quad (1)$$

where m_p stands for the four-dimensional Planck mass and $g_{\mu\nu}$ for the components of the four-dimensional metric

$$ds^2 = dt^2 - a^2(t)d\mathbf{x}^2, \quad (2)$$

which we shall consider to be a homogeneous, isotropic,

and spatially flat Friedman-Robertson-Walker (FRW) cosmology, as supported by recent data [2].

S_{sources} stands for the classical action describing the physical energy content, such as matter and radiation, but it could also include more exotic sources (e.g. defects, cosmic strings, etc.). Note also that we have implicitly assumed the existence of a single canonically normalized quintessence scalar field $q(t, \vec{x})$ subject to the potential $V(q)$. Thus, we have assumed that this potential is independent of the derivatives of the scalar field. For generality, in Eq. (1) we include the effect of higher derivative terms in the gravitational sector of the theory [8]. These are described by the function $f(R, R^{\mu\nu}R_{\mu\nu}, \ldots)$ of the different invariants that we can construct out of the metric and its derivatives. In four dimensions, the most general lowest order corrections to Einstein's classical action would be described by $f = \beta R^2 + \delta R^{\mu\nu}R_{\mu\nu}$[1] (see, for example, [34]). Other corrections that have been considered, include arbitrary functions of the scalar curvature $f(R)$ [35], which include as particular examples linear combinations of negative powers of these invariants [36].

We focus on cosmologies given by Eq. (2), and shall restrict ourselves to classical configurations $q = q(t)$, configurations that do not break the homogeneity and isotropy of spacetime. The energy momentum tensor of this scalar field configuration is that of a perfect fluid, with density ρ_q and pressure p_q given by

$$\rho_q = K(q) + V(q), \qquad p_q = K(q) - V(q),$$
$$\text{and} \quad K \equiv \frac{1}{2}\dot{q}^2, \quad (3)$$

where K denotes the kinetic energy of the field. Under these assumptions, one is led to consider Einstein's equations, plus the Klein-Gordon equation of motion for the scalar field. The first ones reduce to Friedmann's equations

$$H^2 = \frac{\kappa}{3}(\rho_T + \rho_q),$$
$$\frac{\ddot{a}}{a} = -\frac{\kappa}{6}(\rho_T + 3p_T + \rho_q + 3p_q), \quad (4)$$

where $\kappa = 8\pi/m_p^2$ (or $\kappa = 8\pi G$). In Eq. (4) we introduced the compact notation ρ_T and p_T for the total energy density and pressure. For example ρ_T denotes the full energy density contribution of S_{sources} and of the higher derivative curvature terms $f(R, R^{\mu\nu}R_{\mu\nu}, \ldots)$. Thus if the sources are a collection of n perfect fluids with constant equation of state ω_i $i = 1, \ldots, n$, ρ_T, and p_T are

$$\rho_T = \sum_{i=1}^{n} \rho_i + \rho_f, \qquad p_T = \sum_{i=1}^{n} \omega_i \rho_i + p_f, \quad (5)$$

---

[1]These are corrections that are known to be generated by quantum corrections to the classical action, and, in particular, the ones considered here involve a linear combination of the set of independent operators of lowest dimension.

where ρ_f and p_f describe the contribution from the higher derivative curvature terms. For the particular function $f(R^2, R^{\mu\nu}R_{\mu\nu})$ introduced above, such terms would be written as

$$\kappa\rho_f = -12H\frac{a^{(3)}}{a}(3\beta + \delta) - 6\left(\frac{\ddot{a}}{a}\right)^2(3\beta - \delta)$$
$$+ 6H^4(15\beta + 7\delta) - 36H^2\frac{\ddot{a}}{a}(\beta + \delta),$$

$$\kappa p_f = 4\frac{a^{(4)}}{a}(\delta + 3\beta) + 12H\frac{a^{(3)}}{a}(\delta + 2\beta) + 8H^2\frac{\ddot{a}}{a}(\delta$$
$$+ 9\beta) + 2\left(\frac{\ddot{a}}{a}\right)^2(\delta + 3\beta) + 2H^4(15\beta + 7\delta).$$

On the other hand, the scalar field $q(t)$ equation of motion reduces to

$$\ddot{q} + 3H\dot{q} + V' = 0, \qquad (6)$$

where $V' = dV/dq$.

B. Reconstruction procedure

In this section we provide exact analytical expressions in which both the kinetic and potential energies of the quintessence field $q(t)$ depend on quantities more directly observable such as the energy densities, the Hubble constant H, and its derivatives. Although the higher curvature corrections are not directly observable, they will also have to appear in the expressions: they can be taken into account for a given model, that is for a given parametrization of the functional f. Provided one has an independent way of determining the densities H and $\dot{H}$ the value of the potential $V(z)$ at a given redshift z where these measurements are available, can then be fixed, up to experimental uncertainties. If also higher-order derivatives of H are known, higher derivatives of the potential $\frac{d^{(s)}V}{dq^{(s)}}(z)$ can be determined, which can be used to probe the flatness of the potential.

We use the analogous of the inflationary *horizon-flow parameters* [32,33] $\{\varepsilon_n\}$, which are defined recursively by

$$\varepsilon_{n+1} = \frac{d\log|\varepsilon_n|}{dN}, \qquad n \geq 0$$

where $N = \log(a(t)/a(t_i))$ is the number of e-foldings since some initial time t_i and $\varepsilon_0 = H(N_i)/H(N)$. There are many similarities between the period of inflation and the presentday accelerated expansion, but, despite the fact that inflation happened 13.7×10^9 years ago, and the accelerated expansion is happening today, as we will see, it is not observationally easier to reconstruct the dark energy potential than it is to reconstruct the inflationary potential. In the equation describing inflationary dynamics the contribution due to matter can be ignored, but it cannot be ignored when describing today's expansion. Moreover, the detailed shape of the primordial power spectrum from cosmic microwave background (CMB) scales to large scale

structure scales, and the nature of the primordial perturbations offer a window to test the last 4 inflation e-foldings; conversely, in the case of dark energy, dark energy started dominating at $z < 1$, and between then and now the Universe expanded only by a factor <2. In addition we can measure with exquisite precision perturbations from inflation but have not detected perturbations from dark energy, which is a very challenging task [37]. On the other hand we do not have strong constraints on the energy scale of inflation, that is on the "normalization" of the inflationary potential [38,39] but as we will see, since the matter content of the Universe can be independently determined, for a flat Universe, we have some constraints on the quintessence potential normalization.

Keeping in mind the different kind of challenges that a quintessence potential reconstruction faces, we proceed with our program. For our purposes, it will be useful to have explicit expressions for the first two parameters

$$\varepsilon_1 = -\frac{\dot{H}}{H^2} = 1 - \frac{\ddot{a}}{a}H^{-2} = \frac{dH}{dz}\frac{(1 + z)}{H}, \qquad (7)$$

$$\varepsilon_2 = \frac{\dot{\varepsilon}_1}{H\varepsilon_1}, \qquad (8)$$

which, we will show, are needed to determine V and V'.[2] We use the second Friedmann equation (4) to express the first horizon-flow parameter ε_1 in terms of the energy and pressure densities:

$$\varepsilon_1 = \frac{3}{2}\frac{\rho_T + \rho_q + p_T + p_q}{\rho_T + \rho_q}. \qquad (9)$$

If we write $\{\rho_q, p_q\}$ in terms of its kinetic and potential energy components, as in (3), we can use (9) to express, e.g., the kinetic energy in terms of the potential energy as

$$\frac{1}{2}\dot{q}^2 = \frac{1}{3 - \varepsilon_1}\left\{\varepsilon_1(\rho_T + V) - \frac{3}{2}(\rho_T + p_T)\right\}. \qquad (10)$$

Finally we can use the first Friedmann Eq. (4) to solve for the value of the kinetic energy and the potential at a given redshift z

$$K(z) = \frac{1}{2}\dot{q}^2 = \varepsilon_1\frac{H^2}{\kappa} - \frac{1}{2}(\rho_T + p_T), \qquad (11)$$

$$V(z) = (3 - \varepsilon_1)\frac{H^2}{\kappa} + \frac{1}{2}(p_T - \rho_T). \qquad (12)$$

This is the generalization of Eq. (16) in [33] which was derived in the context of inflation.

Equation (12) is a general and exact reconstruction formula for the potential of a quintessence field given the assumptions followed in this paper. As example of the generality of this approach, one can see that it can accom-

---

[2]Throughout this paper we denote with ' the derivative with respect to q and with ˙ derivative with respect to time.

modate models containing nontrivial interactions between matter and the quintessence field [40] simply by replacing $\rho_m(z)$ by $\rho_m(z)g(q(z))$ where $g(q)$ describes the nontrivial interaction.

It is also straightforward to include modifications to General Relativity, as mentioned above. Remarkably, due to the fact that any modification to General Relativity that only depends on the scalar curvature, that is $f = f(R)$, is equivalent to a single scalar field coupled to gravity in a potential determined by the function $f(R)$ and its derivatives [35], our formalism could be used to put constraints on such modifications.

Here, we shall focus in the constraints on the dark energy potential at redshifts smaller than 1000. Therefore, we shall neglect the radiation energy density contribution. Furthermore, if we also neglect the contribution from the higher-order curvature terms, the expression for the potential simplifies

$$V(z) = (3 - \varepsilon_1)\frac{H^2}{\kappa} - \frac{1}{2}\rho_m. \tag{13}$$

Analogously, for the kinetic energy we obtain

$$K(z) = \varepsilon_1 \frac{H^2}{\kappa} - \frac{1}{2}\rho_m. \tag{14}$$

Ideally, our goal would be to constrain the functional form of the potential $V[q]$, and this is not what (12) provides. If the function $q(z)$ was known this would be straightforward, but $q(z)$ is *not* an observable quantity. We will show later (in II C) how $V[q]$ can be obtained.

We can next determine the first derivative with respect to the field of the quintessence potential. We rewrite (6) as

$$V' = -(\dot{q})^{-1}\{3H\dot{q}^2 + \dot{q}\,\ddot{q}\}, \tag{15}$$

where all terms are already known, except for $\dot{q}\,\ddot{q}$ which can be obtained from the time derivative of the kinetic energy (11). The end result can be expressed as

$$V\prime = -3\frac{mp}{\sqrt{4\pi}}H^2(\varepsilon_1)^{1/2}\left\{1 - \frac{\kappa}{2H^2\varepsilon_1}[\rho T + pT]\right\}^{-1/2}$$
$$\times \left\{1 + \frac{\varepsilon 2}{6} - \frac{\varepsilon 1}{3} - \frac{\kappa}{6H3\varepsilon_1}\left[3H(\rho T + pT)\right.\right.$$
$$\left.\left. + \frac{1}{2}(\dot{\rho}T + \dot{p}T)\right]\right\}. \tag{16}$$

Thus, if the values of $\rho_T(z)$, $p_T(z)$, and $\{H, \varepsilon_1, \varepsilon_2\}$ or equivalently, $\{H, \dot{H}, \ddot{H}\}$, can be experimentally determined for some redshift z, II B yields the first derivative of the potential $V'(z)$. As in the previous discussion, the determination of $V'[q(z)]$ would require the knowledge of $q(z)$.

The above formula is the exact result given some energy density content ρ_T, with associated pressure p_T. If we restrict ourselves to a single matter component and neglect the higher-order curvature terms, the first potential derivative reduces to

$$V'(z) = -3\frac{m_p}{\sqrt{4\pi}}H^2(\varepsilon_1)^{1/2}\left\{1 - \frac{\kappa}{2H^2\varepsilon_1}\rho_m\right\}^{-1/2}$$
$$\times \left\{1 + \frac{\varepsilon_2}{6} - \frac{\varepsilon_1}{3} - \frac{\kappa}{4H^3\varepsilon_1}\rho_m\right\}, \tag{17}$$

and (17) reproduces Eq. (17) in [33] when the matter density vanishes ($\rho_m = 0$).

In this case, the first derivative of the potential $V'(z)$ is known if one can measure $\rho_m, \{H, \dot{H}, \ddot{H}\}$. In the absence of coupling between matter and the quintessence field $\rho_m(z = 0)$ is needed instead of $\rho_m(z)$.

Analogously, exact expressions for higher-order derivatives of the potential $d^{(r)}V[q]/dq^r$ can be obtained by taking the time derivative of II B and using the exact expression for the kinetic energy (11). In section V we will use the values of V and V' to find the conditions that the potential has to satisfy to be a natural generalization of the slow-roll conditions during inflation, including the effects of matter.

C. Redshift parametrization of the potential

In section II B we have shown that an exact reconstruction of $V(z)$ is possible only if $H(z)$ and $\dot{H}(z)$ are known. While the determination $H(z)$ is an observationally challenging task (e.g, [28–30,41] and section IV), the determination of $\dot{H}(z)$ is even more formidable.

In this section we shall not attempt a nonparametric and exact reconstruction of $V(z)$, we shall instead consider a parametric description of the potential ($V(\alpha_i, z)$) in terms of the redshift z and parameters α_i. In section IV we will then use currently available observations to constrain the potential parameters and discuss future prospects. Hereafter we will set $\rho_f \equiv 0$ and defer the more general case of $\rho_f \neq 0$ to future work.

Equation (13) can be rewritten in terms of the independent variable z as

$$3H^2(z) - \frac{1}{2}(1 + z)\frac{dH^2(z)}{dz} = \kappa\left(V(\alpha_i, z) + \frac{1}{2}\rho_m(z)\right)$$
$$\equiv g(\alpha_i, z). \tag{18}$$

This is a first-order nonlinear differential equation which can be integrated analytically:

$$H^2(\alpha_i, z) = H_0^2(1 + z)^6 - 2(1 + z)^6$$
$$\times \int_0^z g(\alpha_i, x)(1 + x)^{-7}dx$$
$$= \left(H_0^2 - \frac{\kappa}{3}\rho_{m,0}\right)(1 + z)^6 + \frac{\kappa}{3}\rho_m(z) - 2(1 + z)^6$$
$$\times \int_0^z V(\alpha_i, x)(1 + x)^{-7}dx. \tag{19}$$

Hereafter the 0 subscript denotes the quantity evaluated at $z = 0$.

In this approach if we now consider the kinetic energy of the quintessence field we obtain a first-order nonlinear differential equation for $q(z)$

$$\frac{1}{2}(\dot{q})^2 = (1 + z)^6 V_0 - 6(1 + z)^6 \int_0^z V(\alpha_i, z)(1 + z)^{-7} dz$$
$$+ K_0(1 + z)^6 \qquad (20)$$

or equivalently

$$\frac{1}{2}\left(\frac{dq}{dz}\right)^2 (1 + z)^2 H^2(\alpha_i, z) = 3\kappa^{-1} H^2(\alpha_i, z) - \rho_m(z)$$
$$- V(\alpha_i, z), \qquad (21)$$

which can be integrated to obtain $q(z)$ and thus $V[\alpha_i, q]$ from $V(\alpha_i, z)$:

$$q(z) - q(0) = \pm \int_0^z \frac{dz}{(1 + z)H(\alpha_i, z)} \{6\kappa^{-1}H^2(\alpha_i, z)$$
$$- 2\rho_m(z) - 2V(\alpha_i, z)\}^{1/2}, \qquad (22)$$

where the ambiguity in sign comes from the quadratic expression for the kinetic energy. Typically, if we think of a scalar field rolling slowly along its potential, the plus sign will be the relevant one.

Thus the approach highlighted here enables one to go from determinations of observable quantities $\rho_m(0)$ and $H(z)$ to a reconstruction of the dark energy potential V as a function of the field q without taking time or redshift derivatives. This is of relevance because not $V(z)$ but $V(q)$ is a quantity that can be more directly related to theory but which is not directly observable.

For example let us consider a simple two-parameter parametrization of the potential:

$$V = \lambda(1 + z)^\alpha, \qquad (23)$$

which yields

$$H^2(z) = H_0^2(1 + z)^6 - 2I_\alpha(1 + z)^6, \qquad (24)$$

where

$$I_\alpha = -\frac{\kappa}{6}\rho_m(0)[(1 + z)^{-3} - 1]$$
$$+ \frac{\lambda\kappa}{\alpha - 6}[(1 + z)^{\alpha-6} - 1], \qquad (25)$$
$$\alpha \neq 6$$

$$I_6 = -\frac{\kappa}{6}\rho_m(0)[(1 + z)^{-3} - 1] + \lambda\kappa \log(1 + z),$$
$$\alpha = 6. \qquad (26)$$

If we can neglect the kinetic energy (that is if $\alpha \ll 1$) then this potential corresponds to a constant equation of state w: $\alpha = 3(w + 1)$ as in the Ratra-Peebles [3] case and $\Omega_{q,0} = 6\lambda/[\rho_c(6 - \alpha)]$. In general $V(q)$ can be obtained integrating Eq. (22) with substitutions (23) and (24).

D. Chebyshev reconstruction

An interesting parametrization of the potential involves the Chebyshev polynomials, which form a complete set of orthonormal functions on the interval $[-1, 1]$. They also have the interesting property to be the minimax approximating polynomial, that is, the approximating polynomial which has the smallest maximum deviation from the true function at any given order. We can thus approximate a generic $V(z)$ as

$$V(z) \simeq \sum_{n=0}^N \lambda_n T_n(x), \qquad (27)$$

where T_n denotes the Chebyshev polynomial of order n and we have normalized the redshift interval so that $x = 2z/z_{\text{max}} - 1$; z_{max} is the maximum redshift at which observations are available and thus $x \in [-1, 1]$. Since $|T_n(x)| \leq 1$ for all n for most applications, an estimate of the error introduced by this approximation is given by λ_{N+1}. With this parametrization, the relevant integral in (20) becomes:

$$\int_0^z V(y)(1 + y)^{-7} dy = \frac{z_{\text{max}}}{2} \sum_{n=0}^N \lambda_n$$
$$\times \int_{-1}^{2z/z_{\text{max}}-1} T_n(x)(a + bx)^{-7} dx$$
$$\equiv \sum_{n=1}^N \lambda_n F_n(z), \qquad (28)$$

where $a = 1 + z_{\text{max}}/2$ and $b = z_{\text{max}}/2$. These integrals can be solved analytically for any order n as shown in the appendix: F_n are known analytic functions which are reported in the Appendix.

We obtain:

$$H^2(z, \lambda_i) = (1 + z)^6 H_0^2 \left[1 - 3z_{\text{max}} \sum_{n=0}^N \frac{\lambda_n}{\rho_c} F_n(z) \right.$$
$$\left. - \Omega_{m,0}\left(1 - \frac{1}{(1 + z)^3}\right) \right], \qquad (29)$$

where ρ_c denotes the presentday critical density.

Equation (29) seems to describe the potential with $N + 1$ parameters ($\lambda_0 \cdots \lambda_N$). However, since we assume a flat Universe, $\Omega_{m,0}$ constrains the coefficients of the Chebyshev polynomials in expansion (27) and the kinetic energy of the field. For example, if the potential is constant (i.e in a cosmological constant case) then it is completely described by only one parameter λ_0, and since $\dot{q} = 0$, $V_0 + K_0 = V_0 = \rho_{q,0} = \Omega_{q,0}\rho_c$, we have that $\lambda_0 = \Omega_{q,0}\rho_c$. However if the potential is not constant we obtain

$$\frac{1}{2}\dot{q}^2 = V_0(1+z)^6 - V(z) - 6(1+z)^6$$

$$\times \int_0^z V(z)(1+z)^{-7}dz + K_0(1+z)^6$$

$$= V_0(1+z)^6 - V(z) - 3(1+z)^6 z_{\max}\sum_n \lambda_n F_n$$

$$+ K_0(1+z)^6 \qquad (30)$$

and since $V_0 = \sum_{i=0}^N \lambda_i(-1)^n$ we have the constraint:

$$\sum_{i=0}^N \lambda_i(-1)^n + K_0 = \Omega_{q,0}\rho_c. \qquad (31)$$

Once the Chebyshev coefficients are known, Eq. (22) enables one to reconstruct $q(z)$. The $q(z)$ reconstruction together with Eq. (27) can then be used to constrain $V(q)$.

In section IV we show the constraints that can be obtained for the first few Chebyshev coefficients from currently available data.

III. EQUATION OF STATE

It is widespread to parametrize dark energy not by the scalar field potential but by its equation of state. In this section we connect the two descriptions. We first review the relationship between the dark energy density scaling with redshift, the dark energy equation of state, and the dark energy potential. We then apply the reconstruction method of Sec. II D to the dark energy equation of state and compare models presented in the literature with our parametrization.

A. Time-dependent density scaling

Standard contributions to the energy momentum tensor in Einstein's equations are characterized by a parameter that governs how their energy densities decrease with the expansion of the Universe. For the energy density of the scalar field we can write in all generality

$$\rho_q(t) = \rho_q(0)\left(\frac{a_0}{a(t)}\right)^{\gamma(t)}. \qquad (32)$$

The Klein-Gordon equation (6) can be expressed as the conservation equation for the energy momentum tensor describing the scalar field

$$\dot{\rho}_q + 3H(\rho_q + p_q) = 0. \qquad (33)$$

Thus, the pressure of the scalar field $p_q(t)$ can be expressed as a function of the time-dependent exponent $\gamma(t)$

$$p_q(t) = \left[\frac{\gamma(t)-3}{3} - \frac{1}{3}\log\left(\frac{a_0}{a(t)}\right)H^{-1}\frac{d\gamma}{dt}\right]\rho_q(t). \qquad (34)$$

Using ansatz (32), we obtain the kinetic and potential energies for the scalar field

$$\frac{1}{2}\dot{q}^2 = \frac{1}{2}\rho_q(t)\Delta w_q, \qquad (35)$$

$$V = \rho_q\left(1 - \frac{1}{2}\Delta w_q(t)\right), \qquad (36)$$

where we introduced the function (compare to [42])

$$\Delta w_q(t) = \frac{1}{3}\left[\gamma(t) - H^{-1}\log\left(\frac{a_0}{a(t)}\right)\frac{d\gamma}{dt}\right], \qquad (37)$$

which depends on the ratio between kinetic and potential energies of the scalar field via

$$\Delta w_q(t) = \frac{2}{1 + V[q]/K[q]}. \qquad (38)$$

The function $\Delta w_q(t)$ controls the deviations from the equation of state of the scalar field $w_q(t)$ from being exactly -1, i.e. a cosmological constant. Indeed, from $p_q(t) = w_q(t)\rho_q(t)$, we have

$$w_q(t) = -1 + \Delta w_q(t). \qquad (39)$$

Thus constraining $\Delta w_q(t)$ is equivalent to constraining the time (or redshift) evolution of the dark energy equation of state for which there are different independent observational constraints (e.g., [3,43], and references therein).

We can relate $\gamma(t)$ to $\Delta w_q(t)$ by integrating (37). Without losing generality, we do this in terms of the redshift

$$\gamma(z) = \frac{3}{\log(1+z)}\int_0^z \Delta w_q(y)\frac{dy}{1+y}, \qquad (40)$$

where we did not include a possible integration constant, since it is physically irrelevant, i.e. it just redefines the value of the energy density of the scalar field today ($\rho_q(0)$). This relation provides an expression for the potential energy density of the scalar field once the equation of state is known, using (36):

$$V(z) = \rho_q(0)e^{3\int_0^z \Delta w_q(y)\frac{dy}{1+y}}\left(1 - \frac{1}{2}\Delta w_q(z)\right). \qquad (41)$$

The case of a constant Δw_q, or equivalently, a constant equation of state w_q would correspond to the redshift parametrization considered in (23) with

$$\lambda = \rho_q(0)\left(1 - \frac{1}{2}\Delta w_q\right), \quad \text{and} \quad \alpha = 3(1 + w_q).$$

Thus, for a physical situation resembling a cosmological constant ($w_q \sim -1$), the parameter $\alpha \ll 1$, as we claimed in the previous section. Some constant scalar field energy density scalings were discussed by [4]. The above formalism is a natural generalization of their models.

B. Beyond a rolling scalar field

Up to now we have assumed that dark energy is given by a scalar field. The techniques developed here however can also be used in a more general context.

If the dark energy is not due to a scalar field we can still describe it as a fluid with a given equation of state. As long as the equation of state w is > -1 the two descriptions are equivalent. For example for a given set of parameters λ_i and H_0 and $\Omega_{m,0}$, $V(\lambda_i, z)$ is known, the kinetic energy can be computed using Eq. (31), thus Δw is known (Eq. (38)) and so $w(z)$ (Eq. (39)).

However if we want to allow $w < -1$ then the scalar field description as presented here fails. However, analogously to section II D, we can expand the redshift dependence of w in Chebyshev polynomials without imposing any restrictions on the values that w can take. We thus obtain

$$w(z) \simeq \sum_{i=0}^{N} \omega_i T(x(z)) \tag{42}$$

and

$$H^2(\omega_i, z) \simeq H_0^2 (1+z)^3$$
$$\times \left[\Omega_{m,0} + \Omega_{q,0} \exp\left(\frac{3}{2} z_{\max} \sum_{n=0}^{N} \omega_n G_n(z) \right) \right], \tag{43}$$

where G_n is the analogous of F_n of section II D: F_n is a linear combination of integrals I_i, $i = \{0, n\}$ while G_n is the same linear combination of the integrals J_i, $i = \{0, n\}$ (see the appendix).

Note that in this parametrization the presentday value of w is given by

$$w_0 = \sum_{i=0}^{N} (-1)^i \omega_i. \tag{44}$$

Given the parametrization (42) of $w(z)$ subject to the constraint $w > -1$ one can always obtain:

$$V(z) = \rho_{q,0}(1+z)^{3(1+\omega_0)} \exp\left[\frac{3}{2} z_{max} \sum_{i=1}^{N} \omega_i G_i(z) \right]$$
$$\times \frac{1}{2} \left[1 - \sum_{i=0}^{N} \omega_i T_i(x(z)) \right]. \tag{45}$$

In section IV we show how currently available data can be used to constrain the first few Chebyshev coefficients of this expansion.

In the remaining of this section we will compare some models presented in the literature with the parametrization presented here. Clearly, the case of a constant equation of state corresponds to $\omega_i = 0$ for $i > 0$. The linear parametrization in z [44,45] corresponds to $\omega_i = 0$ for $i > 1$, and in particular $w_0 = \omega 0 - \omega_1$ and $w' = 2\omega_1/z_{\max}$. Finally the linear parametrization in a [46,47], $w = w_0 +$ $w_a z/(1+z)$ for $w_a \ll w_0$ can be closely approximated by $\omega_i = 0$ for $i > 2$, with the constraint (44). [48] pointed out that a simple, 2-parameter fit may introduce biases: the expansion (42) allows one to include more parameters by increasing N as the observational data improve.

IV. OBSERVATIONAL DETERMINATION OF $H(z)$

Section II B has illustrated that it is necessary to determine observationally $H(z)$, $\dot{H}(z)$, $\ddot{H}(z)$ in order to reconstruct $V[q]$ and its first derivative $V'[q]$.

[28–30] pointed out that the first derivative with respect to redshift of the "coordinate distance" y (where y is related to the luminosity distance d_L by $d_L = 1/H_0 y(1+z)$) can yield a measurement of $H(z)$ and $\rho_q(z)$ and that if one also has knowledge of the second derivative, one can obtain constraints on $p(z)$ and $w(z)$. They then propose a robust numerical differentiation technique where observational determinations of $y(z)$ are binned and approximated in each bin by a second-order polynomial; the derivatives are then obtained for each bin from the best fit coefficients of the polynomial. They thus obtain a piecewise reconstruction of $H(z)$, $\rho_q(z)$, $p_q(z)$, and $w(z)$ for data sets comprised of luminosity distances to type IA supernovae and coordinate distances to radio galaxies. In principle the potential could be reconstructed from these quantities.

Here we also start off by presenting a determination of $H(z)$. Our determination is based on the method developed by [49] and it uses measurements of relative ages of passively evolving galaxies. Since the systematic errors in spectroscopic dating of galaxies tend to cancel out when computing relative ages, we deem this a robust method to obtain $H(z)$ directly from data. We briefly discuss the reliability of this $H(z)$ determination and possible issues, but a detailed comparison of reliability and performance of the two different approaches will be discussed elsewhere.

We emphasize the difficulties of computing $\dot{H}(z)$, $\ddot{H}(z)$, necessary to reconstruct not just the potential itself but also higher-order derivatives of the potential $d^n V/dq^n$. We also present the constraints that can be achieved on the evolution of the quintessence potential and the dark energy equation of state from present and future data.

A. Sample selection and differential ages of passively evolving galaxies

The Hubble parameter depends on the differential age of the Universe as a function of redshift in the form

$$H(z) = -\frac{1}{1+z} \frac{dz}{dt}. \tag{46}$$

Therefore a determination of dz/dt directly measures $H(z)$. In [41] we demonstrated the feasibility of the method by applying it to a $z \sim 0$ sample. In particular, we used the Sloan Digital Sky Survey to determine $H(0)$ and showed

that its value is in good agreement with other independent methods (see [41] for more details). With the availability of new galaxy surveys it becomes possible to determine $H(z)$ at $z > 0$. Here we use the new publicly released Gemini Deep Survey (GDDS) survey [50] and archival data [51–56] to determine $H(z)$ in the redshift range $0.1 < z < 1.8$. We proceed as follows: first we select galaxy samples of passively evolving galaxies with high-quality spectroscopy. Second, we use synthetic stellar population models to constrain the age of the oldest stars in the galaxy (after marginalizing over the metallicity and star formation history), in similar fashion as is done in [41]. We compute *differential* ages and use them as our estimator for dz/dt, which in turn gives $H(z)$.

The first sample is composed of field early-type galaxies from [51–53]. In [41] we selected galaxies from [51–53] to obtain a sample of old elliptical galaxies with high signal to noise (S/N) spectra and we derived ages for this sample using the SPEED models [57]. Here from this sample we discard galaxies for which the spectral fit indicates an extended star formation, that is for which the best fit declining exponential has a decaying time greater than 0.1 Gyr. This leaves us with 10 galaxies.

The second sample is composed by 20 old passive galaxies ([58]) from the publicly released GDDS [50]. GDDS has high-quality spectroscopy of red galaxies, some of which show stellar absorption features, indicating an old stellar population. The GDDS collaboration has determined ages (and the star formation history) for these galaxies [58]: they conclude that for a subsample of 20 red galaxies the most likely star formation history is that of a single burst of star formation of duration less than 0.1 Gyr (in most cases the duration of the burst is consistent with 0 Gyr, i.e. the galaxies have been evolving passively since their initial burst of star formation). To determine the galaxies ages they use a set of stellar population models different than SPEED. We have reanalyzed the GDDS old sample using SPEED models and obtained ages within 0.1 Gyr of the GDDS collaboration estimate. This indicates that systematics are not a serious source of error for these high-redshift galaxies. We complete our data set by adding the two radio galaxies 53W091 and 53W069 [54–56] which are the reddest radio galaxies in the Windhorst *et al.* survey. In total we have 32 galaxies.

Figure 1 (left panel) shows the estimated *absolute* ages for galaxies in the above samples and their 1σ error bars. There is a distinguishable "red envelope": galaxies are older at lower redshifts.

The next step is to compute differential ages at different redshifts from this sample. To do so we proceed as follows: first we group together all galaxies that are within $\Delta z = 0.03$ of each other. This gives an estimate of the age of the Universe at a given redshift with as many galaxies as possible. The interval in redshift is small to avoid incorporating galaxies that have already evolved within the bin, but large enough for our sparse sample to have more than
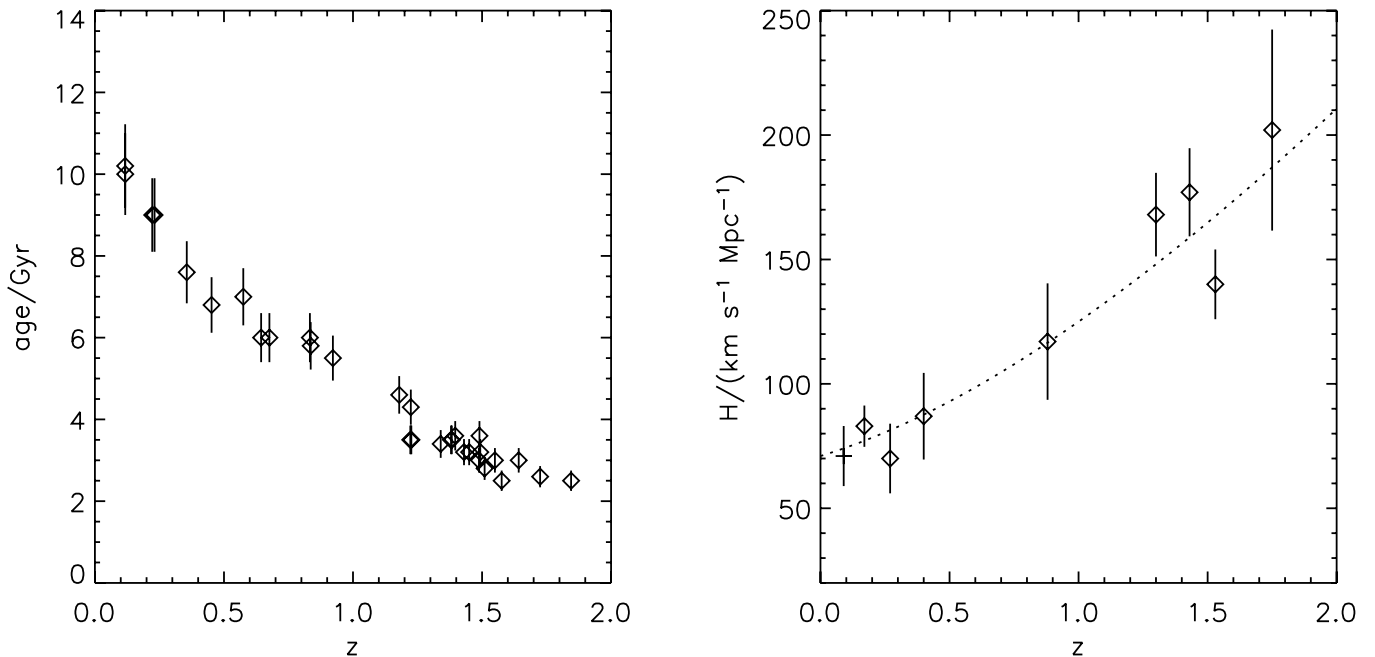

FIG. 1.   Left panel: the absolute age for the 32 passively evolving galaxies in our catalogue (see text for more details) determined from fitting stellar population models is plotted as a function of redshift. Note that there is a clear age-redshift relation: the lower the redshift the older the galaxies. Right panel: the value of the Hubble parameter as a function of redshift as derived from the *differential* ages of galaxies in the left panel. The determination at $z \sim 0.1$ indicated by the '+' symbol is the Hubble constant determination of H from [41]. The dotted line is the value of $H(z)$ for the LCDM model.

one galaxy in most of the bins. Then for each bin we discard those galaxies that are more than 2σ away from the oldest galaxy in that bin.

We then compute age differences only for those bins in redshift that are separated more than $\Delta z = 0.1$ but no more than $\Delta z = 0.15$. The first limit is imposed so that the age evolution between the two bins is larger than the error in the age determination. We find that this provides a robust determination of dz/dt since the recovered dz/dt depends weakly on the choice of binning. With this procedure we obtain 8 determinations of $H(z)$.

We note here that differential ages are less sensitive to systematics errors than absolute ages (see [57] for detailed discussion, especially their table 2). The value of $H(z)$ is then directly computed by using Eq. (46). This is shown in Fig. 1 with 1σ error bars. Also shown (dotted line) is $H(z)$ for the lambda cold dark matter (LCDM) model.

Before we can use these data to derive constraints on dark energy we need to be aware of the effects of potential systematic uncertainties of the method. This has been somewhat discussed in [41] for the Treu sample, but we review it briefly here and extend it to the rest of the set. Ages were obtained assuming a single-burst stellar population model and a single metallicity model. For the GDDS galaxies [58] performed fits for declining star formation histories and for the 20 galaxies we use the best fitting model corresponded to that of a single burst (declining

exponential time less than 0.1 Gyr). This supports using the single-burst model. The high quality of the GDDS spectra allows us to explore different star formation histories concluding that the single burst is the one best fitting the models.

While the single metallicity approximation affect the recovered ages well below the error bars, the single-burst approximation may not work as well in general. In fact it is known that massive elliptical galaxies can experience some level of star formation activity at low redshift. This can bias the single-burst equivalent ages of the spectrum towards younger ages. Although this is a serious caveat for the interpretation of individual galaxy spectra our selection is designed to keep only the oldest galaxies in each redshift bin. However we do rely on having a fair sample of the galaxy population in each redshift bin so that even though the ages for some galaxies will scatter towards younger ages, it is still possible to find enough galaxies to define the so-called "red envelope." Since our method relies on the shape of the "red envelope," it is insensitive to any systematic shift in the ages determinations as long as the shift is constant with redshift. On the other hand our results could potentially be seriously compromised if the determination of the "red envelope" was affected in a redshift-dependent way. While there is no intrinsic reason for this to happen, observational and selection effects can in principle do that but we are not aware of it.
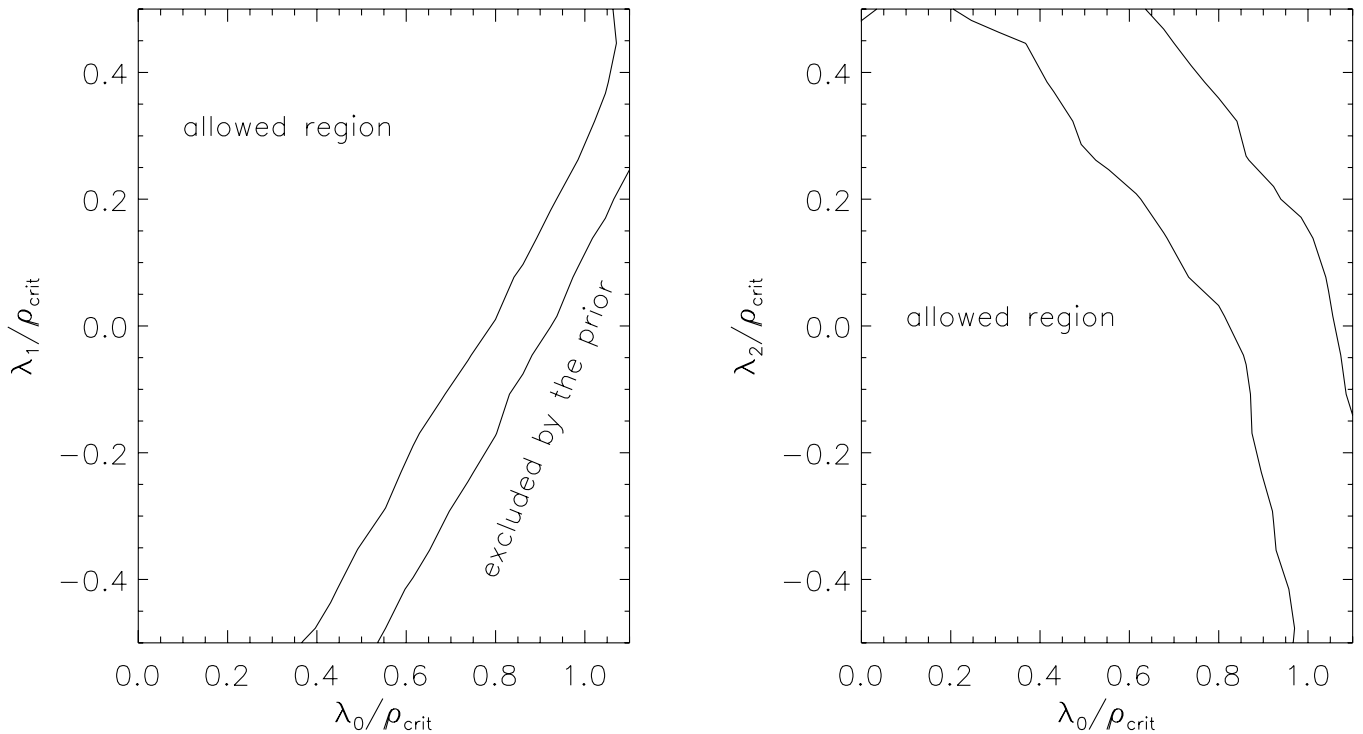

FIG. 2.   Regions in the λ_1/ρ_c vs λ_0/ρ_c (left panel) and λ_2/ρ_c vs λ_0/ρ_c (right panel) excluded at the 1σ and 2σ joint confidence level, by the priors and the constraints that the kinetic energy in the quintessence field must be positive and that at all redshifts $\rho_m + \rho_q$ must be positive.

B. Constraints on the potential

Following the discussion in sec. II D, we present constraints on the shape of the potential achievable from present and future data sets. Figure 3 shows the constraints on the first three Chebyshev coefficients for the potential that can be obtained from our galaxy sample, combined with the determination of the Hubble constant at $z = 0.09$ obtained by [41] from the Sloan digital sky survey (SDSS) luminous red galaxies. We have assumed a flat Universe and marginalized over a Gaussian prior on $\Omega_{m,0}$ ($\Omega_{m,0} = 0.27 \pm 0.07$ (e.g., [59]) and a flat prior on H_0 ($30 < H_0 < 100$ Km/s/Mpc). We have used only the large scale structure prior on $\Omega_{m,0}$, as the determination of [59] is insensitive to dark energy. Conversely, CMB constraints on the matter density of the Universe are highly sensitive to the assumptions about the nature of dark energy (see e.g., [2] in particular figure 12), and thus should not be used in this context. Of course, the addition of CMB data can greatly improve the constraints on the nature of dark energy, but this needs to be done in a joint analysis and it is left for future work.

Some regions of the parameter space are unphysical as they would yield a negative kinetic energy or $\rho_m + \rho_q < 0$; the combined effect of these priors in the λ_1/ρ_c vs λ_0/ρ_c plane and λ_2/ρ_c vs λ_0/ρ_c plane is shown in Fig. 2. We consider only the region $0 < \lambda_0/\rho_c < 1.1$, $-0.5 < \lambda_1/\rho_c < 0.5$, and $-0.5 < \lambda_2/\rho_c < 0.5$.

In Fig. 3 we show the one and 2 sigma joint confidence contours in the λ_0/ρ_c vs λ_1/ρ_c and λ_0/ρ_c vs λ_2/ρ_c planes, obtained from our $H(z)$ determination. When adding the Hubble space telescope (HST) key project prior on H_0 [60] the contours remain virtually unchanged. For comparison in Fig. 4 we show the constraint obtained by using the recent supernovae data of [1].

Figure 5 shows our best fit reconstructed $V(z)$ from our $H(z)$ determination (left panel) and from the SN data (right panel), and the 68% and 95% confidence regions. The present constraints are consistent at the 1-σ level with a constant potential (that is the cosmological constant scenario).

The two determinations (one based on relative galaxy ages and one SN data) are consistent with each other. The two methods are completely independent and are based on different underlying physics, different assumptions, and affected by systematics of completely different nature. The fact that they agree indicates that possible systematics are smaller than the statistical errors.

With current data there is a degeneracy between the first two coefficients, but we can place an upper limit to the kinetic energy in the quintessence field today: the contribution of the kinetic term to ρ_q is less than 40% at the 2-σ level and the best fit value is at 0. For completeness in Fig. 6 we report the reconstructed potential as a function of the field.
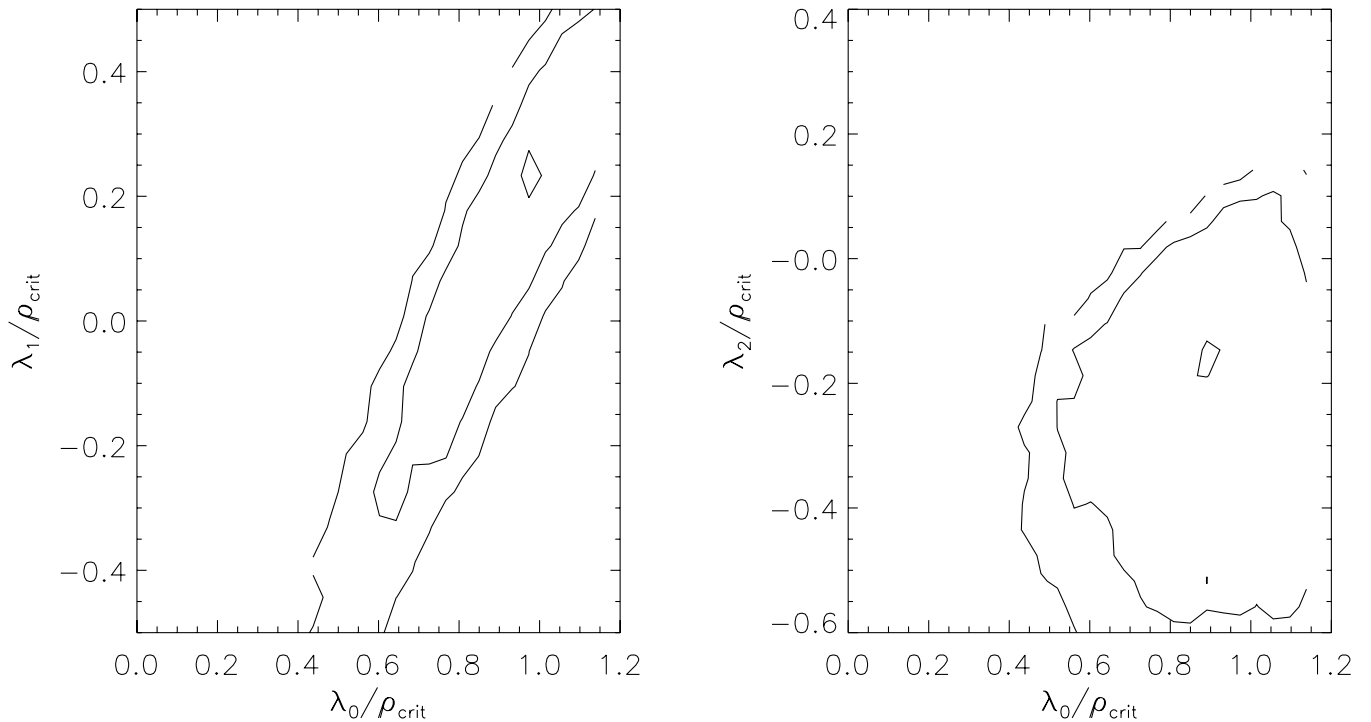

FIG. 3.   Constraints in the λ_1/ρ_c vs λ_0/ρ_c (left panel) and λ_2/ρ_c vs λ_0/ρ_c (righ panel) obtained from $H(z)$ measurement based on relative galaxy ages. Contour levels are 1σ marginalized, 1σ joint, and 2σ joint. The diamond shows the location of the maximum of the marginalized likelihood.
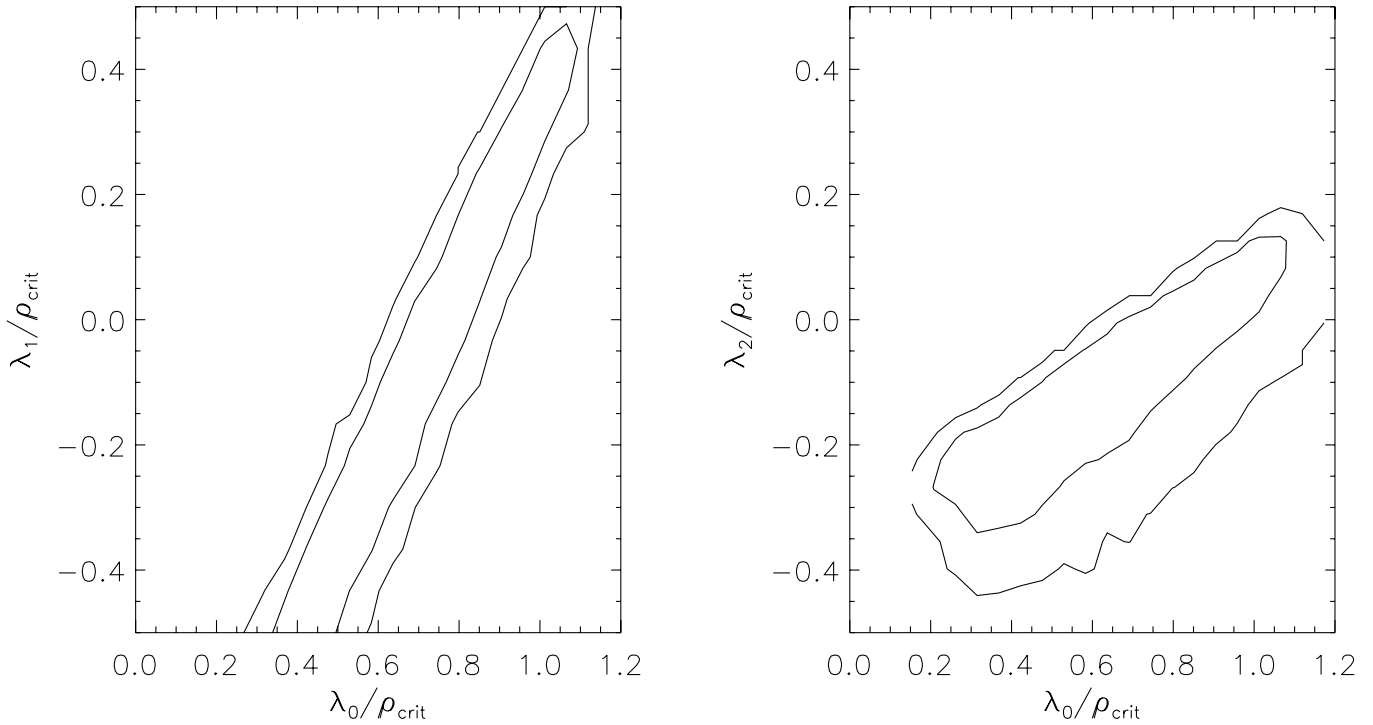
FIG. 4. One and two sigma joint constraints in the λ_1/ρ_c vs λ_0/ρ_c plane and λ_2/ρ_c vs λ_0/ρ_c obtained from the Riess *et al.* (2004) supernovae data.

The Atacama Cosmology Telescope (ACT: [61] www.hep.upenn.edu/act) will identify, through their Sunyaev-Zeldovich signature in the cosmic microwave background, all galaxy clusters with masses $>10^{14}$ M$_\odot$ in a patch of the sky of angular size 100 square degrees. Thus ACT will yield $\gtrsim 500$ galaxy clusters in the redshift range $0.1 < z < 1.5$. For all these clusters, spectra of the brightest galaxies in the cluster will be obtained by South
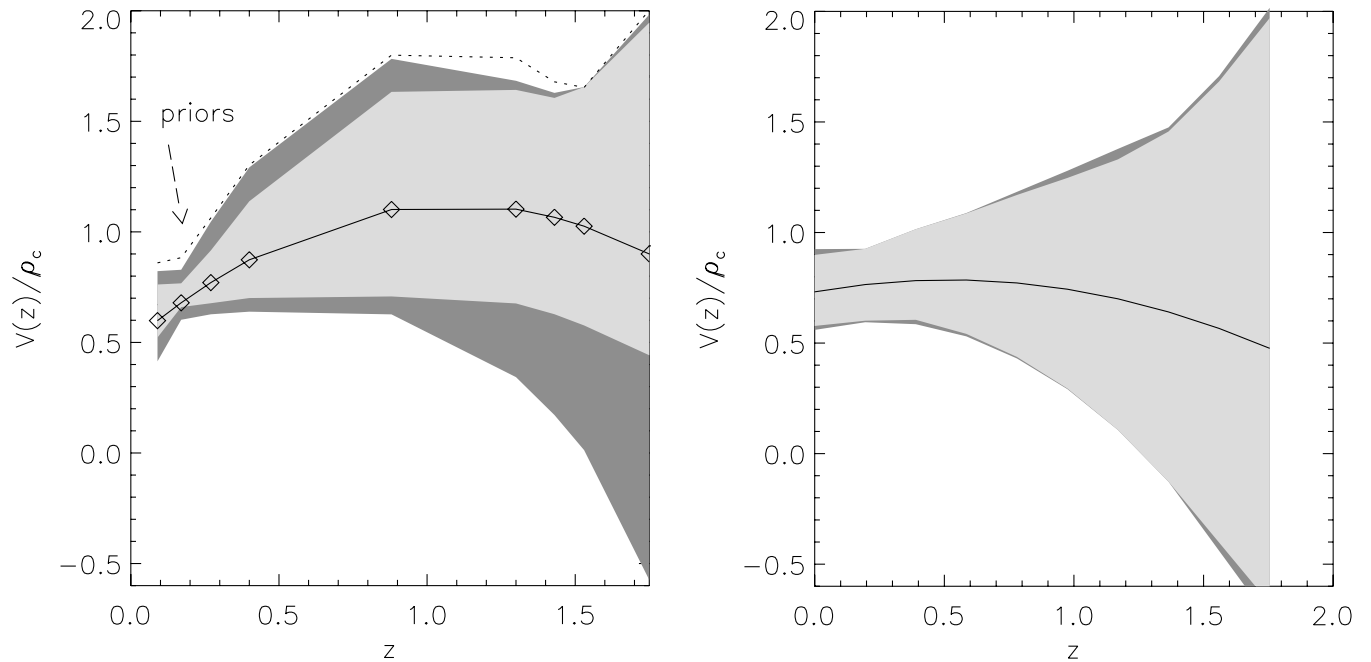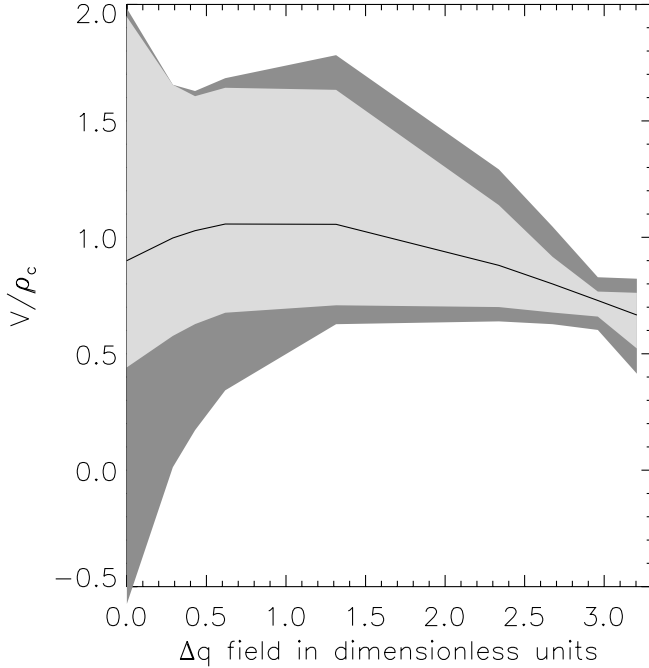

FIG. 5. Reconstructed $V(z)$ from relative galaxy ages (left) and from Supernovae (right). The gray regions represent the 1 and 2σ confidence regions. In the left panel the dotted line shows the constraint imposed by the prior.

FIG. 6.   Reconstructed $V(q)$ from relative galaxy ages.

African and Chilean telescopes. This will provide us with an unbiased sample of $\gtrsim 2000$ passively evolving galaxies from $z = 1.5$ to the present day. To estimate the performance of ACT galaxies at reconstructing the dark energy potential, we have estimated that we will have 2000 galaxies for which ages have been determined with $\sim 10\%$ accuracy and therefore ~ 1000 determinations of h with $\sim 15\%$ error. Our[3] forecasts in the reconstruction of the dark energy potential are shown in Fig. 7. We have marginalized over a flat prior on the Hubble constant $30 < H_0 < 90$ km s $^{-1}$Mpc^{-1} and a Gaussian prior on $\Omega_{m,0}$, $\Omega_{m,0} = 0.27 \pm 0.035$, as an estimate of the improvement of this determination from galaxy surveys.

C. Constraints on the equation of state

It is illustrative to work out the consequences of the constraints found on λ_0, λ_1, λ_2. Let us consider the potential (23) that gives rise to a constant equation of state. If α is small then one can approximate the potential with $\lambda(1 + \alpha z)$ and thus identify the coefficients in the Chebyshev expansion: $\lambda_0 \longrightarrow \lambda$ and $\lambda_1 \longrightarrow \lambda\alpha$, $\lambda_2 = 0$. We thus obtain $\lambda_1/\lambda_0 < 0.3$ at the 1-σ level; since $\lambda_1/\lambda_0 \simeq \alpha = 3(w + 1)$ we obtain $w \lesssim -0.9$ at the 1-σ level.

As illustrated in Sec. III B for more general cases we can expand the redshift evolution of the equation of state parameter in terms of Chebyshev polynomials. Here we show how constraints on $w(z)$ obtained from our galaxy

---

[3]L. V. and R. J. are members of the ACT science team and plan to apply this technique to ACT data when available in $\sim$2006-2007.

sample with the differential ages method compare with other constraints. For example in Fig. 8 (left panel) we show the constraints in the plane ω_0 vs ω_1 (i.e. we impose $N = 1$ in (42)), where we have used the HST key prior for H_0 and the prior $\Omega_{m,0} = 0.27 \pm 0.04$ as in [1]. The contours show the 1σ marginalized, 1σ, and 2σ joint confidence levels. To compare with the SN constraints of [1] recall that their w_0 is $\omega_0 - \omega_1$. Thus the degeneracy seen in the figure is a constraint on w_0. Three points in the ω_0 vs ω_1 parameter space are indicated by the diamond, star, and '+' sign. These points are at the 1σ joint confidence level, well within the 1σ marginalized level and at the 1σ marginalized level, respectively. In particular the '*' point corresponds to the LCDM model. In the right panel we show the difference between the Hubble parameter for a given model and that in the LCDM case. Also our determinations of $H(z)$ are shown. The long-dashed line corresponds to the LCDM case (* point), the dot-dashed line corresponds to the "diamond"-point and the dot-dot-dot-dashed line to the '+'-point. It is clear that more datapoints in the redshift range around $z = 0.7$ would help in breaking the degeneracy.

V. SLOW-ROLL DARK ENERGY

The constraints derived from our observational determination of $H(z)$ combined with our theoretical analysis suggest that observations in the redshift range $0.1 < z < 1.8$ are consistent, at the 1σ level, with a cosmological constant equation of state ($w = -1$).

This suggests to analyze more closely the conditions under which a quintessence field could resemble such an equation of state in that redshift range, because this is the challenge we will be facing in the near future.

There are at least two different approaches that one can attempt: either work with a generic potential and determine the properties it has to satisfy to resemble a cosmological constant, or attempt to argue some universality in the functional form of the potential due to its expected flatness in field space.

A. Slow roll in redshift

Given a generic potential scalar field in the presence of a non-negligible matter energy density $\rho_m(z)$, we would expect the conditions the potential has to satisfy to be a natural generalization of the slow-roll conditions during inflation, including the effects of matter. These two conditions are:

$$w_q(z) \approx -1, \qquad \frac{dw_q(z)}{dt} \approx 0, \qquad \forall z \in [0, z_0]. \quad (47)$$

The first one ensures that dark energy behaves approximately as a cosmological constant at a given redshift z, whereas the second ensures that such property is maintained in time.
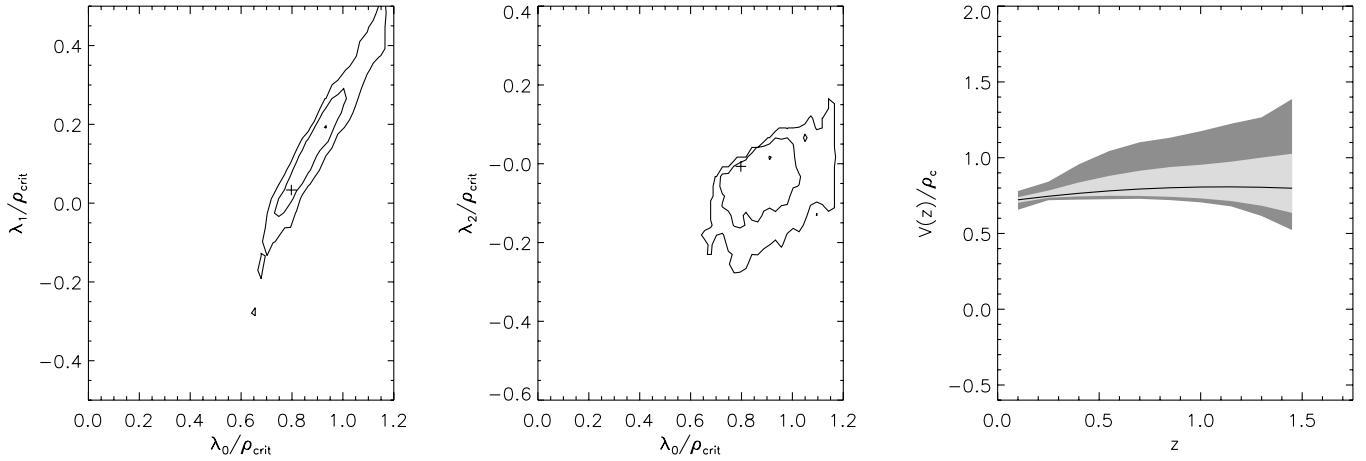
FIG. 7.   Predicted constraints for an experiment with 2000 galaxies for which ages are measured with an accuracy of ∼10%. The constraint in the Chebyshev coefficients (left panels; circles show the location of the maximum marginalized likelihood while '+' show the location of the maximum of the joint 5D likelihood) and the reconstructed dark energy potential (right panel) are significantly better than current constraints (see text). We have a LCDM model as fiducial. The Atacama Cosmology Telescope will identify about 500 galaxy clusters in the redshift range $0.1 < z < 1.5$, for at least 2000 galaxies there will be spectroscopic follow-up and therefore galaxy ages can be derived.

There are several equivalent ways of studying the consequences of these conditions. In terms of the kinetic scalar field energy $K[q]$ and its potential energy $V[q]$, Eq. (47) implies that $V[q] \gg K[q]$ and that the ratio, $K[q]/V[q]$ is nearly constant in time:

$$w_q(z) \approx -1 \quad \Rightarrow \quad \frac{K[q]}{V[q]} \ll 1,$$
$$\frac{dw_q(z)}{dt} \approx 0 \quad \Rightarrow \quad \frac{dK[q]/V[q]}{dt} \approx 0. \tag{48}$$

In terms of the fundamental degrees of freedom $q(t)$, conditions (47) are equivalent to

$$w_q(z) \approx -1 \quad \Rightarrow \quad \frac{1}{2}\dot{q}^2 \ll V[q], \tag{49}$$

$$\frac{dw_q(z)}{dt} \approx 0 \quad \Rightarrow \quad \frac{\ddot{q}}{V'[q]} \approx \frac{K[q]}{V[q]} \ll 1, \tag{50}$$

where the last inequality is derived from the identity

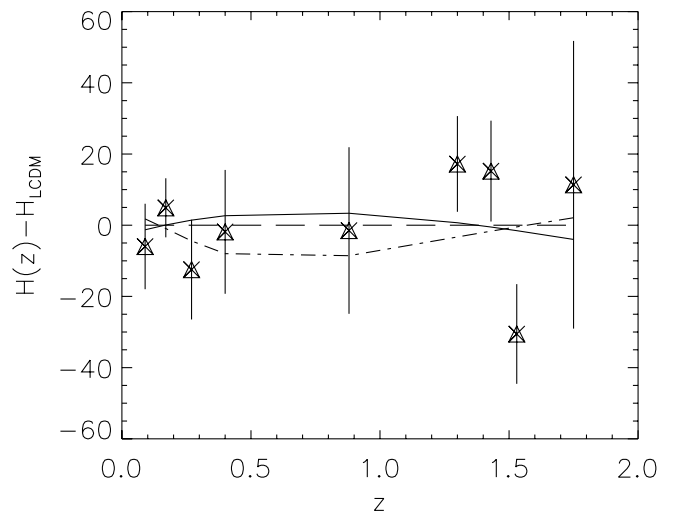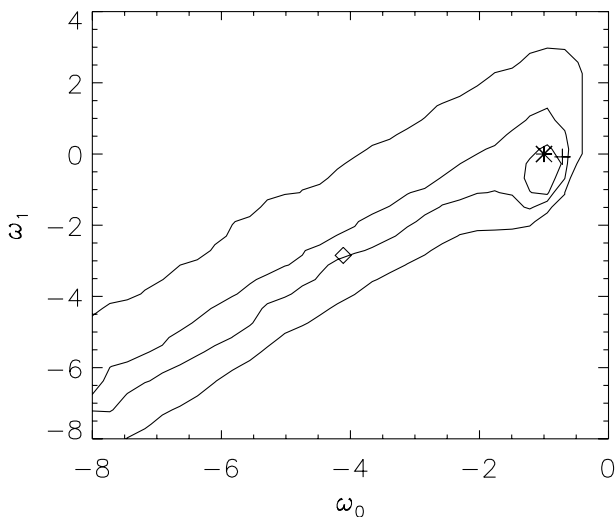FIG. 8.   Left panel: Constraints in the ω_0 vs ω_1 obtained from our galaxy sample with the differential ages method. The contours show the 1σ marginalized, 1σ, and 2σ joint confidence levels. The degeneracy constrains $w_0 \equiv \omega_0 - \omega_1$. Three points in the parameter space are selected. Right panel: difference between the Hubble constant in a given model and the Hubble constant in the LCDM model. The points with error bars are our data points, the long-dashed line corresponds to the LCDM model (*-point in the left panel), the dot-dashed line corresponds to the diamond-point, and the dot-dot-dot-dashed one to the '+'-point.

$$\frac{dw_q}{dt} = 2\frac{\dot{q}V[q]}{\rho_q^2}\left\{\ddot{q} - \frac{K[q]}{V[q]}V'[q]\right\}. \qquad (51)$$

Under these circumstances, the first Friedmann equation (4) and the Klein-Gordon equation (6) reduce to

$$3\frac{H^2}{\kappa} \approx \rho_m + V, \qquad 3H\dot{q} \approx -V', \qquad (52)$$

which are the extension of the slow-roll equations used in inflation in the presence of matter. One can now rewrite conditions (49) and (50), respectively as

$$\left(\frac{m_p V'}{V}\right)^2 \ll 48\pi\left(1 + \frac{\Omega_m}{\Omega_q}\right), \qquad (53)$$

$$m_p^2 \frac{V''}{V} \ll 24\pi\left(1 + \frac{3}{2}\frac{\Omega_m}{\Omega_q}\right), \qquad (54)$$

where we already used the fact that $\rho_m V^{-1} \sim \Omega_m \Omega_q^{-1}$ whenever (49) is satisfied.

Following the discussion in section II C, it is also convenient to rewrite these conditions in terms of redshift derivatives of the potential $V[q(z)]$. The analogue of conditions (53) and (54) are:

$$\frac{1}{V}\frac{dV}{dz} \ll \frac{6}{1+z}, \qquad (55)$$

$$\left(\frac{dV}{dz}\right)^{-1}\frac{d^2V}{dz^2} \ll \frac{5}{1+z}. \qquad (56)$$

B. Slow roll in the field

Phenomenologically, there are many inequivalent functionals that could be chosen to describe the quintessence field dynamics. Each of them would typically depend on a set of undetermined parameters, which would be determined by fitting them to observations, as we did in Section IV. In order for a generic potential to look indistinguishable from a cosmological constant, these parameters need to be highly fine-tuned.

It is precisely this fine-tuning that suggests that, *independently* of the functional form of the potential, the potential will allow an expansion in terms of the variation of the unobservable scalar field variation $\Delta_q(t) = q(t) - q(0)$, measuring its variation from its current value today.

Let us assume that there is a certain period of physical time around today, i.e. $t = 0$, and consistent with the range of redshift covered in this work, where the variations in the scalar potential are small in field space. In other words, the potential is "flat." Under these conditions, and independently of its functional form, the potential $V[q]$ can be approximated by

$$V[q] \approx V[q(0)] + V'[q(0)]\Delta_q(t) + \frac{1}{2}V''[q(0)](\Delta_q(t))^2 + \mathcal{O}((\Delta_q(t)))^3). \qquad (57)$$

Let us emphasize that such an expansion is always viable for small enough Δ_q, but the Taylor expansion can have a wider validity if the potential is flat enough, that is if the derivatives of the potential are small $|V^n| \ll V_0$ and if the kinetic energy is small $K \ll V_0$.

For this to be a good approximation the following two conditions should be satisfied:

$$\frac{1}{2}V_0''(q(t) - q(0)) \ll V_0', \qquad (58)$$

$$V_0'(q(t) - q(0)) < V_0, \qquad (59)$$

where we introduced the notation $V_0^{(n)} = \frac{d^n V[q]}{dq^n}[q(0)]$.

We shall also assume that the energy of the scalar field $q(t)$ is dominated by the potential energy

$$\frac{1}{2}\dot{q}^2 \ll V[q], \qquad (60)$$

so that the scalar field dynamics can resemble a cosmological constant (see (48)) and the rolling due to the kinetic energy is small. In the following, we shall proceed to attempt to integrate the system perturbatively. At zeroth order in the potential expansion the first of Friedmann's equation in (4) reduces to

$$H^2 \sim \frac{\kappa}{3}\left(\rho_{T,0}\left(\frac{a_0}{a}\right)^{3(1+w)} + V_0\right),$$

where $a(0) \equiv 1$. If $\rho_{T,0} = \rho_{m,0}$, $w = 0$ and this reduces to the case of a LCDM universe.

The exact solution

$$3H = \frac{2c}{1+w}\frac{y_0 + \tanh ct}{1 + y_0\tanh ct}, \qquad (61)$$

and

$$(a(t))^{3(1+w)} = (\cosh ct)^2(1 + y_0\tanh ct)^2, \qquad (62)$$

becomes, for matter + dark energy universe

$$a(t)^3 = (y_0^2 - 1)\sinh^2(ct + \hat{c}), \qquad (63)$$

which yields a Hubble parameter, at zeroth-order $H(t)^{-1} = 3\tanh(ct + \hat{c})/(2c)$, where we have introduced two dimensionless parameters:

$$y_0 = \sqrt{\frac{\rho_0}{V_0} + 1}, \qquad \tanh\hat{c} = y_0^{-1}, \qquad (64)$$

and the dimensional one

$$c = \sqrt{3\kappa V_0}\frac{1+w}{2}. \qquad (65)$$

In a matter + dark energy universe ($w = 0$) and in our

current approximation $c \sim 3H_0\sqrt{\Omega_{q,0}}/2 \sim 0.09$ Gyr^{-1}, whereas $y_0 \sim \sqrt{\Omega_{m,0}/\Omega_{q,0} + 1} \sim 1.18$ and $\hat{c} \sim 1.2$. Thus the age of the Universe is ~ 13 Gyrs.

We can then proceed to integrate the Klein-Gordon equation by taking the first nontrivial contribution coming from the expansion (57), and plugging in the zeroth-order Hubble parameter

$$\ddot{q} + 3H\dot{q} + V_0' \sim 0. \qquad (66)$$

The solution for the velocity of the scalar filed is

$$\dot{q} = \frac{k - F(t)}{(\cosh ct + y_0 \sinh ct)^{2/(1+w)}}, \qquad (67)$$

where

$$F(t) = V_0' \int_0^t [\cosh cx + y_0 \sinh cx]^{2/(1+w)} dx$$

$$= (\text{if } w = 0) \frac{1}{2c} V_0'(y_0^2 - 1)$$

$$\times \left(\frac{1}{2} \sinh 2(ct + \hat{c}) - (ct + \hat{c}) \right). \qquad (68)$$

Here, k is the integration constant and we have used the fact that $y_0^2 - 1 > 0$ and the identity

$$\cosh ct + y_0 \sinh ct = \sqrt{y_0^2 - 1} \sinh(ct + \hat{c}). \qquad (69)$$

Note that we could identify the constant of integration k with the expression $k = \dot{q}(0) + F(0)$ involving the kinetic energy of the scalar field today. A second further integra-

FIG. 9. Interval in time where the slow-roll approximation is valid for some choices of V_0' and K_0, when $V_0/\rho_c = 0.7$.

tion yields the dynamical evolution for the field

$$q(t) - q(0) = k_1 + k \int^t (a(x))^{-3} dx - \int^t F(x)(a(x))^{-3} dx, \qquad (70)$$

which in a matter + dark energy universe becomes

$$q(t) - q(0) = \frac{k}{c(y_0^2 - 1)\tanh\hat{c}} \left(1 - \frac{\tanh\hat{c}}{\tanh(ct + \hat{c})} \right)$$

$$+ \frac{V_0'}{2c^2} \left(\frac{\hat{c}}{\tanh\hat{c}} - \frac{ct + \hat{c}}{\tanh(ct + \hat{c})} \right), \qquad (71)$$

where

$$k = \dot{q}(0) + F(0), \qquad F(0) = (y_0^2 - 1)\frac{V_0'\hat{c}}{2c} \left(\frac{\sinh 2\hat{c}}{2\hat{c}} - 1 \right). \qquad (72)$$

The approximations presented here are therefore valid if $V_0'/V_0[q(t) - q(0)] < 1$. Figure 9 shows, for some choices of V_0, V_0', and K_0, the range in lookback time where this approximation is valid.

VI. CONCLUSIONS

We have proposed to constrain the nature of dark energy, a rolling scalar field, or a cosmological constant, by reconstructing its potential as a function of redshift. We have presented a formalism, similar to the horizon-flow parameters in inflation, to relate quantities characterizing the dark energy dynamics, i.e. potential and kinetic energy densities, to direct observables such as the matter density $\rho_m(z)$, the Hubble parameter $H(z)$, and its derivatives. This is the core of our reconstruction programme, and our results are summarized by (12), (11), and (16), which provide the value of the potential and kinetic energy densities, and the first derivative of the potential, as a function of redshift. These expressions are valid even in the presence of higher-order curvature corrections to General Relativity and exotic matter sources. In principle, integrating the exact reconstruction formula for the kinetic energy, allows one to determine the function $q(z)$. Using the latter, one can infer the real shape of the potential $V[q]$ from the determination of $V(z)$.

We have then focused on the case of an expanding universe with only matter and dark energy components and at $z \ll 1000$. In this case the above expressions simplify to (13), (14), and (17). These exact reconstruction formulas are currently difficult to be used due to the experimental challenges in determining the derivatives of the Hubble parameter IV. However, given a parametrization for the potential energy density, the relation (18) becomes a differential equation for the Hubble parameter which can be integrated analytically. Thus determinations of $H(z)$ can be used to constrain $V(z)$ directly. Since effectively one will always be dealing with observations covering a finite redshift range, by an appropriate linear
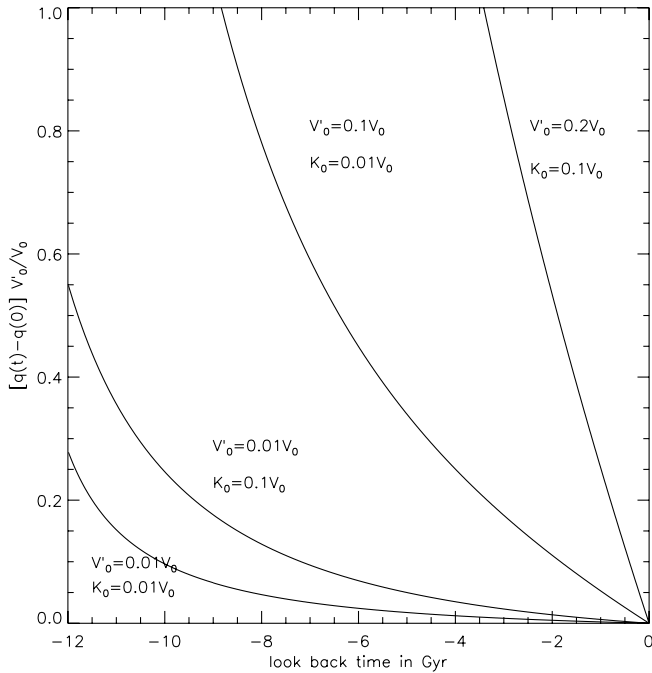
transformation in the redshift variable, we can always work in the interval $[-1, 1]$, where we know the set of Chebyshev polynomials provide a complete orthonormal set of functions, i.e. any function in the interval can be expressed as a linear combination of Chebyshev polynomials. Moreover, these approximating polynomials have the smallest maximum deviation from the true function at any given order, and provide a well-defined estimate of the error introduced in the truncation of the expansion at a finite order. We point out, in passing, that such a parametrization could be used in any other attempts considered in the literature where it was the equation of state the observable being parametrized by its redshift dependence.

Using observations of passively evolving galaxies we obtain measurements of the Hubble parameter at 9 different redshifts. We use these determinations to constrain the first three coefficients in the Chebyshev expansion of the potential. For comparison we repeat the analysis using recent supernovae data, which give us an integral of the Hubble parameter. We find that the reconstructed potentials from both data sets are consistent, giving some confidence that the results are not heavily plagued by systematic errors. The standard LCDM model is consistent with current data at the 1σ level. We show that future data obtained from the Atacama Cosmology Telescope will greatly improve the constraints.

Since a cosmological constant is a good fit to the observations we asked the question of how to generically describe small deviations from this simple scenario. It is clear that even if the nature of dark energy might be related to a dynamical field, distinguishing such a scenario from a real cosmological constant will be an extraordinary experimental challenge, as the dark energy potential can be arbitrarily close to a constant.

We thus analyzed the conditions for the dark energy field to "slow roll" in the presence of matter, thus enabling a dynamical dark energy to get arbitrarily close to a cosmological constant (47). By expanding the potential in Taylor series for $\Delta_q(t) = q(t) - q(0)$ we derived the generalization of the standard slow-roll conditions used in inflation, in the presence of matter, which translate into conditions that the functional $V[q]$ must satisfy to explain the maximum deviation allowed from a cosmological constant.

Even though in this paper we focused on single canonically normalized scalar field, it should be clear that it is straightforward to apply our formalism to an arbitrary number of them, not necessarily being canonically normalized. However, the observables quantities are the matter density, the Hubble parameter, and its derivatives, which depend on the full kinetic and potential energy densities of the scalar field sector, and are insensitive to whether these values are given by the superposition of more than one field. This poses the question of whether one would be able to determine, experimentally, the existence of more than one rolling scalar field. In other words, "to which extent it

is possible to disentangle the full kinetic/potential energy of a superposition of scalar fields into the kinetic/potential energies of their components?"

We have illustrated the enormous experimental challenges of reconstructing $V[q]$ from $V(z)$ just for a single scalar field. The task is even harder for more than one field as there are more derivative directions to consider, $\partial V/\partial q_i$, and direct experimental observables depend only on the time derivatives of the full potential energy, i.e. $dV/dt = \partial V/\partial q_i \dot{q}_i$. Such a disentanglement seems extremely challenging, if not impossible, at least from the perspective of the formalism developed here. In this context we can say that our formalism enables one to reconstruct the properties (potential and kinetic energy) of an "effective" field.

APPENDIX A

Chebyshev polynomials can be computed using the recursion relation:

$$T_{n+1}(x) = 2xT_n(x) - T_{n-1}(x) \quad \text{for} \quad n \geq 1, \quad (A1)$$

where

$$T_0(x) = 1, \qquad T_1(x) = x. \quad (A2)$$

Thus $T_n(x)$ will have the following structure: $T_n(x) = \alpha_0 x^n + \alpha_2 x^{n-2} + \alpha_4 x^{n-4} + \ldots$, so for example:

$$T_2(x) = 2x^2 - 1, \qquad T_3(x) = 4x^3 - 3x,$$
$$T_4(x) = 8x^4 - 8x^2 + 1. \quad (A3)$$

The integral on the right-hand side of Eq. (28) will involve a series of integrals of the type:

$$I_n = \int_{-1}^{2z/z_{\max}-1} x^n (a + bx)^{-7} dx. \quad (A4)$$

In particular, using the recursion relation of the Chebyshev polynomials we find that:

$$T_0(x) = 1 \quad \Rightarrow \quad F_0(x) \equiv I_0,$$

$$T_1(x) = x \quad \Rightarrow \quad F_1(x) \equiv I_1,$$

$$T_2(x) = 2x^2 - 1 \quad \Rightarrow \quad F_2(x) \equiv [2I_2 - I_0],$$

$$T_3(x) = 4x^3 - 3x \quad \Rightarrow \quad F_3(x) \equiv [4I_3 - 3I_1],$$

$$T_4(x) = 8x^4 - 8x^2 + 1 \quad \Rightarrow \quad F_4(x) \equiv [8I_4 - 8I_2 + I_0],$$

$$T_5(x) = 16x^5 - 20x^3 + 5x \quad \Rightarrow$$
$$F_5(x) \equiv [16I_5 - 20I_3 + 5I_1],$$

$$T_6(x) = 32x^6 - 48x^4 + 18x^2 - 1 \quad \Rightarrow$$
$$F_6(x) \equiv [32I_6 - 48I_4 + 18I_2 - I_0],$$

where

$$I_n = \left(\frac{2z}{z_{\max}} - 1\right)^{n+1} \left[\frac{1}{6} \frac{(1+z)^{-6}}{a} - \frac{(n-5)(1+z)^{-5}}{30a^2}\right.$$
$$+ \frac{(n-5)(n-4)(1+z)^{-4}}{120a^3} \tag{A5}$$

$$- \frac{(n-5)(n-4)(n-3)(1+z)^{-3}}{360a^4}$$
$$+ \frac{(n-5)\cdots(n-2)(1+z)^{-2}}{720a^5}$$
$$\left. - \frac{(n-5)\cdots(n-1)(1+z)^{-1}}{720a^6}\right] \tag{A6}$$

$$-(-1)^{n+1}\left[\frac{1}{6a} - \frac{(n-5)}{30a^2} + \frac{(n-5)(n-4)}{120a^3}\right.$$
$$\left. - \frac{(n-5)(n-4)(n-3)}{360a^4} + \frac{(n-5)\cdots(n-2)}{720a^5} \right. \tag{A7}$$

$$\left. - \frac{(n-5)(n-1)}{720a^6}\right] + \frac{(n-5)\cdots n}{720a^6} J_n \tag{A8}$$

and

$$J_n = \int_{-1}^{2z/z_{\max}-1} \frac{x^n}{(a+bx)} dx. \tag{A9}$$

These integrals are given by

$$J_n = \sum_{m=0}^{n-1} (-1)^m a^m \frac{[(2z/z_{max} - 1)^{(n-m)} - (-1)^{(n-m)}]}{(n-m)b^{(m+1)}}$$
$$+ (-1)^n \frac{a^n}{b^{(n+1)}} \log(1+z) \tag{A10}$$

but can also be obtained using the recursion relation

$$J_n = \frac{1}{nb}[(2z/z_{\max} - 1)^n - (-1)^n] - \frac{a}{b} J_{n-1}, \tag{A11}$$

where

$$J_0 = \frac{1}{b} \log(1+z). \tag{A12}$$

Integrals I_n can also be obtained by recursive relation [62]

$$I_n = \frac{(1+z)^{-6}(2z/z_{\max} - 1)^n - (-1)^n}{(n-6)z_{\max}/2}$$
$$- \frac{n(1+z_{\max}/2)}{(n-6)z_{\max}/2} I_{n-1} \tag{A13}$$
$$\text{for} \quad n \neq 6,$$

where

$$I_0(x) = -\frac{1}{3z_{\max}}\left(\frac{1}{(1+z)^6} - 1\right). \tag{A14}$$

In the case of Eq. (43) G_n are defined as:

$$T_0(x) = 1 \quad \Rightarrow \quad G_0(x) \equiv J_0,$$

$$T_1(x) = x \quad \Rightarrow \quad G_1(x) \equiv J_1,$$

$$T_2(x) = 2x^2 - 1 \quad \Rightarrow \quad G_2(x) \equiv [2J_2 - J_0],$$

etc.

---

[1] A. G. Riess, L. Strolger, J. Tonry, S. Casertano, H. C. Ferguson, B. Mobasher, P. Challis, A. V. Filippenko, S. Jha, W. Li *et al.*, Astrophys. J. **607**, 665 (2004).

[2] D. N. Spergel, L. Verde, H. V. Peiris, E. Komatsu, M. R. Nolta, C. L. Bennett, M. Halpern, G. Hinshaw, N. Jarosik, A. Kogut *et al.*, Astrophys. J. Suppl. Ser. **148**, 175 (2003).

[3] B. Ratra and P. J. E. Peebles, Phys. Rev. D **37**, 3406 (1988).

[4] B. Ratra and P. J. E. Peebles, Phys. Rev. D **37**, 3406 (1988).

[5] C. Wetterich, Nucl. Phys. B **302**, 668 (1988).

[6] R. R. Caldwell, R. Dave, and P. J. Steinhardt, Phys. Rev. Lett. **80**, 1582 (1998).

[7] G. Huey, L. Wang, R. Dave, R. R. Caldwell, and P. J. Steinhardt, Phys. Rev. D **59**, 063005 (1999).

[8] S. M. Carroll, V. Duvvuri, M. Trodden, and M. S. Turner, Phys. Rev. D **70**, 043528 (2004).

[9] K. Freese and M. Lewis, Phys. Lett. B **540**, 1 (2002).

[10] WMAP: http://.map.gsfc.nasa.gov.

[11] SNAP: http://snap.lbl.gov.

[12] DUO: http://duo.gsfc.nasa.gov.

[13] ACT:[61], http://www.hep.upenn.edu/act.

[14] SPT: http://astro.uchicago.edu/spt.

[15] Planck: http://astro.estec.esa.nl/Planck.

[16] M. Kunz, P. Corasaniti, D. Parkinson, and E. J. Copeland, Phys. Rev. D **70**, 041301 (2004).

[17] P. S. Corasaniti and E. J. Copeland, Phys. Rev. D **65**, 043004 (2002).

[18] M. Tegmark, M. A. Strauss, M. R. Blanton, K. Abazajian, S. Dodelson, H. Sandvik, X. Wang, D. H. Weinberg, I.

Zehavi, N. A. Bahcall *et al.*, Phys. Rev. D **69**, 103501 (2004).

[19] I. Maor, R. Brustein, J. McMahon, and P. J. Steinhardt, Phys. Rev. D **65**, 123003 (2002).

[20] I. Maor and R. Brustein, Phys. Rev. D **67**, 103508 (2003).

[21] M. Jarvis, B. Jain, G. Bernstein, and D. Dolney, astro-ph/0502243.

[22] Y. Wang and P. M. Garnavich, Astrophys. J. **552**, 445 (2001).

[23] Y. Wang and M. Tegmark, Phys. Rev. Lett. **92**, 241302 (2004).

[24] Y. Wang and K. Freese, astro-ph/040220.

[25] Y. Wang, V. Kostov, K. Freese, J. A. Frieman, and P. Gondolo, J. Cosmol. Astropart. Phys. **12**, 3 (2004).

[26] U. Alam, V. Sahni, T. Deep Saini, and A. A. Starobinsky, Mon. Not. R. Astron. Soc. **354**, 275 (2004).

[27] U. Alam, V. Sahni, T. Deep Saini, and A. A. Starobinsky, Mon. Not. R. Astron. Soc. **344**, 1057 (2003).

[28] R. A. Daly and E. J. Guerra, Astron. J. **124**, 1831 (2002).

[29] R. A. Daly and S. G. Djorgovski, Astrophys. J. **597**, 9 (2003).

[30] R. A. Daly and S. G. Djorgovski, Astrophys. J. **612**, 652 (2004).

[31] C. Wetterich, Phys. Lett. B **594**, 17 (2004).

[32] D. J. Schwarz, C. A. Terrero-Escalante, and A. A. Garcia, Phys. Lett. B **517**, 243 (2001).

[33] S. M. Leach, A. R. Liddle, J. Martin, and D. J. Schwarz, Phys. Rev. D **66**, 023515 (2002).

[34] N. D. Birrell and P. C. W. Davies (Cambridge University Press, Cambridge, England, 1982), p. 340.

[35] V. F. Mukhanov, H. A. Feldman, and R. H. Brandenberger, Phys. Rep. **215**, 203 (1992).

[36] S. M. Carroll, V. Duvvuri, M. Trodden, and M. S. Turner, Phys. Rev. D **70**, 043528 (2004).

[37] R. Bean and O. Doré, Phys. Rev. D **69**, 083503 (2004).

[38] H. V. Peiris, E. Komatsu, L. Verde, D. N. Spergel, C. L. Bennett, M. Halpern, G. Hinshaw, N. Jarxosik, A. Kogut, M. Limon *et al.*, Astrophys. J. Suppl. Ser. **148**, 213 (2003).

[39] W. H. Kinney, E. W. Kolb, A. Melchiorri, and A. Riotto, Phys. Rev. D **69**, 103516 (2004).

[40] G. Huey and B. D. Wandelt, astro-ph/0407196.

[41] R. Jimenez, L. Verde, T. Treu, and D. Stern, Astrophys. J. **593**, 622 (2003).

[42] S. Bludman, Phys. Rev. D **69**, 122002 (2004).

[43] W. Hu, astro-ph/0407158.

[44] D. Huterer and M. S. Turner, PRD **64**, 123527 (2001).

[45] J. Weller and A. Albrecht, Phys. Rev. D **65**, 103512 (2002).

[46] M. Chevallier, D. Polarski, and A. Starobinsky, Int. J. Mod. Phys. D **10**, 213 (2001).

[47] E. V. Linder, Phys. Rev. Lett. **90**, 091301 (2003).

[48] B. A. Bassett, P. S. Corasaniti, and M. Kunz, Astrophys. J. Lett. **617**, L1 (2004).

[49] R. Jimenez and A. Loeb, Astrophys. J. **573**, 37 (2002).

[50] R. G. Abraham, K. Glazebrook, P. J. McCarthy, D. Crampton, R. Murowinski, I. Jørgensen, K. Roth, I. M. Hook, S. Savaglio, H. Chen *et al.*, Astron. J. **127**, 2455 (2004).

[51] T. Treu, M. Stiavelli, S. Casertano, P. Møller, and G. Bertin, Mon. Not. R. Astron. Soc. **308**, 1037 (1999).

[52] T. Treu, M. Stiavelli, P. Møller, S. Casertano, and G. Bertin, Mon. Not. R. Astron. Soc. **326**, 221 (2001).

[53] T. Treu, M. Stiavelli, S. Casertano, P. Møller, and G. Bertin, Astrophys. J. Lett. **564**, L13 (2002).

[54] J. Dunlop, J. Peacock, H. Spinrad, A. Dey, R. Jimenez, D. Stern, and R. Windhorst, Nature (London) **381**, 581 (1996).

[55] H. Spinrad, A. Dey, D. Stern, J. Dunlop, J. Peacock, R. Jimenez, and R. Windhorst, Astrophys. J. **484**, 581 (1997).

[56] L. Nolan, J. Dunlop, R. Jimenez, and A. F. Heavens, Mon. Not. R. Astron. Soc. **341**, 464 (2003).

[57] R. Jimenez, J. MacDonald, J. S. Dunlop, P. Padoan, and J. A. Peacock, Mon. Not. R. Astron. Soc. **349**, 240 (2004).

[58] P. J. McCarthy, D. Le Borgne, D. Crampton, H. Chen, R. G. Abraham, K. Glazebrook, S. Savaglio, R. G. Carlberg, R. O. Marzke, K. Roth *et al.*, Astrophys. J. Lett. **614**, L9 (2004).

[59] Verde *et al.*, Mon. Not. R. Astron. Soc. **335**, 432 (2002).

[60] W. L. Freedman, B. F. Madore, B. K. Gibson, L. Ferrarese, D. D. Kelson, S. Sakai, J. R. Mould, R. C. Kennicutt, H. C. Ford, J. A. Graham *et al.*, Astrophys. J. **553**, 47 (2001).

[61] A. Kosowsky, in *The Emergence of Cosmic Structure*, AIP Conf. Proc. No. 666 (AIP, New York, 2003), p. 325.

[62] I. S. Gradshteyn and I. M. Ryzhik, *Table of Integrals, Series and Products*, edited by A. Jeffrey (Academic, New York, 1994), 5th Ed. completely reset.